Pressure effects on the phase transitions and energy gap in CeRhAs

K. Umeo,* K. Masumori, T. Sasakawa, F. Iga, and T. Takabatake
Department of Quantum Matter, ADSM, Hiroshima University, Higashi-Hiroshima 739-8530, Japan

Y. Ohishi and T. Adachi
JASRI/SPring-8, Hyogo 679-5198, Japan
(Received 26 September 2004; published 28 February 2005)

We report on the electrical resistivity, thermal expansion, and x-ray diffraction measurements of single-crystalline sample of the so-called Kondo semiconductor CeRhAs under pressures up to 3 GPa. This compound undergoes successive structural phase transitions at $T_1=360$, $T_2=235$, and $T_3=165$ K at ambient pressure. On cooling below T_1, the crystal structure changes from the hexagonal LiGaGe-type to the orthorhombic ε-TiNiSi-type with a $2b\times 2c$ superlattice. By applying pressure up to 1.5 GPa, T_1 increases with a ratio of 270 K/GPa, whereas both T_2 and T_3 decrease with -100 K/GPa. The concurrent decrease of both the a parameter and the energy gap along the a axis with increasing pressure contradict the c-f hybridization gap model in which the gap is enlarged by the enhancement of hybridization between the $4f$ electrons and conduction band. Instead, a sort of charge-density-wave transition at T_1 is proposed for the origin of gap formation of this compound. The semiconducting behavior in the resistivity vanishes when the phase with the $2b\times 2c$ superlattice decomposes into two orthorhombic phases below 100 K and above 1.5 GPa.

DOI: 10.1103/PhysRevB.71.064110 PACS number(s): 61.50.Ks, 75.30.Mb, 74.62.Fj

I. INTRODUCTION

The ternary Ce compounds CeNiSn, CeRhSb, and CeRhAs, crystallizing in the orthorhombic ε-TiNiSi-type structure have attracted considerable attention, as they possess an anisotropic (pseudo) energy gap near the Fermi level.[1,2] Anisotropic c-f hybridization between the conduction band and $4f$ electrons plays the central role in the gap formation in CeNiSn and CeRhSb.[3] Among these compounds, only CeRhAs undergoes successive structural phase transitions at $T_1=360$ K, $T_2=235$ K, and $T_3=165$ K.[4] With elevating temperature above T_1, the ε-TiNiSi-type structure with a superlattice of modulation vector $q_1=(0\ 1/2\ 1/2)$ changes to a hexagonal LiGaGe-type.[5,6] This structural transition causes a large increase of the orthorhombic a-axis parameter. On cooling below T_1 in reverse, the magnetic susceptibility along all of the principal axes strongly decreases, which suggests the onset of gap formation.[4] Below T_2, two other superlattice reflections appear at $q_2=(0\ 1/3\ 1/3)$ and $q_3=(1/3\ 0\ 0)$. Below T_3, the peak at q_2 suddenly disappears.[6] The rapid increase of electrical resistivity below T_3 indicates the development of the gap. More recently, the analysis of the Hall coefficient indicated that there exist two distinct energy scales for the gap structure; 2000 K below T_1 and 300 K below T_3.[5] These observations imply that the gap formation in CeRhAs is closely related to the lattice modulations, that is, a charge-density-wave (CDW) transition. Furthermore, the excess heat capacity above T_1 from the Dulong-Petit's value might originate from some sort of charge ordering in CeRhAs.[5] On the other hand, the gap magnitude for CeRhSb and CeRhAs derived from the photoemission and electron-tunneling measurements can be scaled with the Kondo temperature $T_K=360$ and 1500 K, respectively, which were estimated by the relation of $T_K\sim 3T_m$, where T_m is the maximal temperature of the magnetic susceptibility.[7,8] The local Kondo coupling tuned by the c-f hybridization is essential for the gap formation. A natural question, then, is the structural phase transitions or the c-f hybridization govern the gap formation in CeRhAs.

Since the c-f hybridization becomes stronger by applying pressure, one expects that the hybridization gap is enlarged. In fact, the magnitude of gap energy for CeRhSb increases with increasing pressure.[9] For polycrystalline CeRhAs, however, the gap was found to be suppressed with increasing pressure above 1.5 GPa.[2] This observation suggests that the gap suppression results from the change of electronic state in this compound. The relation between the structural transitions and stability of the gap has been the issue to be clarified. In this paper, we report the measurements of the resistivity, thermal expansion and x-ray diffraction under pressures for a single crystalline sample. In Sec. II, high pressure techniques are described. In Sec. III, the pressure-temperature phase diagram of CeRhAs is presented, and then the detailed experimental results are described. In. Sec. IV, experimental results will be discussed in relation to the structural phase transitions and gap formation. Finally, the summary and conclusions are given in Sec. V.

II. EXPERIMENTAL PROCEDURE

Single-crystal samples of CeRhAs were grown by the Bridgman technique. The details of preparation and characterization of the sample were described in the previous paper.[4] The electrical resistivity under pressures up to 3 GPa was measured by a dc four-terminal method in the range $0.35\leqslant T\leqslant 520$ K. The thermal expansion was measured by a strain gauge method in the ranges $4.2\leqslant T\leqslant 300$ K and $0\leqslant P\leqslant 2.2$ GPa. A dummy gauge was glued on a Mo plate. The pressure was generated by a clamp-type piston-cylinder pressure cell by using Daphne oil as the pressure transmitting

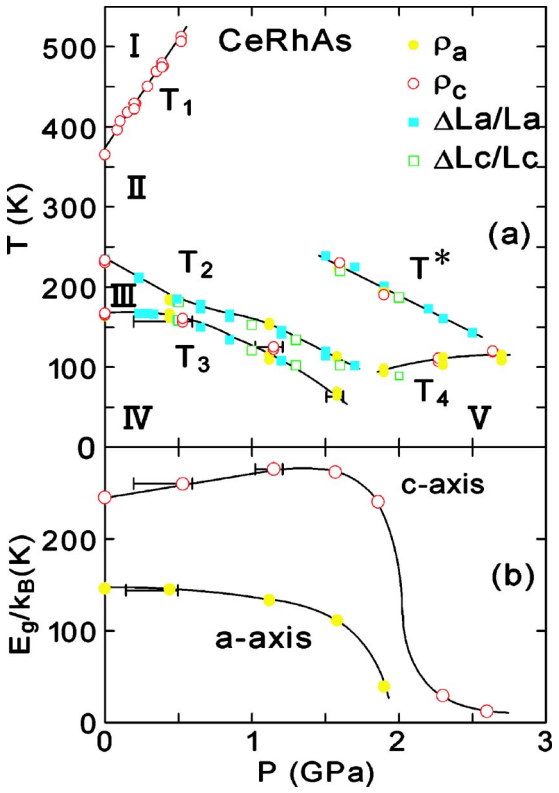

FIG. 1. (Color online) (a) Temperature (T) vs pressure (P) phase diagram of CeRhAs. Solid lines are a guide to the eye. The phases for $T \geq T_1$, $T_1 \geq T \geq T_2$, $T_2 \geq T \geq T_3$, $T_3 \geq T$, and $T_4 \geq T$ are denoted by I, II, III, IV, and V, respectively. (b) Pressure dependence of the energy gap E_g/k_B, which is estimated by the activated behavior for 60 K$<T<$100 K in the electrical resistivity for $I \| a$ and $I \| c$.

medium for the measurements below 300 K. The pressure at room temperature was determined by the change in the resistance of manganin wire, and that at low temperatures by the change in superconducting transition temperature of Sn. For the resistivity measurement above 300 K, silicone oil was used as the transmitting medium, and the load was held at a constant value in the whole temperature range. The x-ray powder diffraction measurements up to 2.5 GPa was carried out by using a diamond anvil cell in BL-10XU, SPring-8.

III. RESULTS

Before presenting the detailed experimental results, the pressure (P) vs temperature (T) phase diagram of CeRhAs is summarized in Fig. 1(a). We call hereafter respective phase as I ($T \geq T_1$), II ($T_1 \geq T \geq T_2$), III ($T_2 \geq T \geq T_3$), and IV ($T_3 \geq T$). With increasing pressure up to 1.5 GPa, both T_2 and T_3 decrease with a ratio of −100 K/GPa, whereas T_1 increases with a ratio of 270 K/GPa. This fact suggests that phase II, where the unit cell of the ε-TiNiSi-type structure is doubled along the b and c axes, is stabilized by applying pressure. As shown in Fig. 1(b), the energy gap E_g/k_B, which is estimated from the activated behavior in the electrical resistivity for $I \| c$ in the range $60 < T < 100$ K, also increases with pressure up to 1 GPa at the initial ratio of 27 K/GPa. Therefore, the

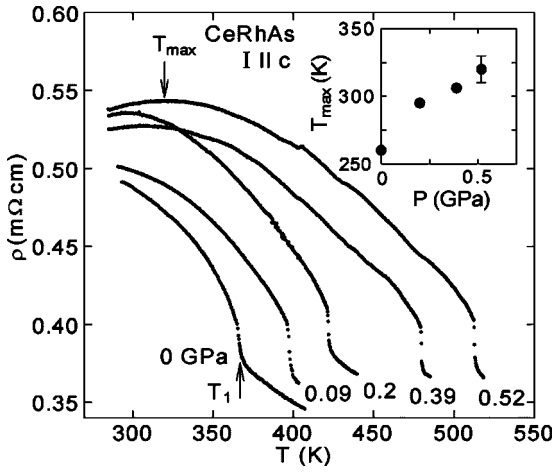

FIG. 2. Electrical resistivity $\rho_c(T)$ along the c axis of CeRhAs for $T>300$ K under pressures up to 0.51 GPa. Inset shows the pressure dependence of the maximal temperature T_{max} in $\rho_c(T)$.

gap along the c axis may be related to the superstructure in the b-c plane. On the other hand, E_g/k_B along the a axis decreases with pressure. For $P>1.8$ GPa, both T_2 and T_3 vanish suddenly and give way to another phase, denoted by phase V, below $T_4 \sim 100$ K. Furthermore, the gap energy for both $I \| a$ and $I \| c$ is strongly suppressed at about 2 GPa. The coincidence between the appearance of phase V and disappearance of the gap suggests that the structural and/or electronic transition below T_4 leads to the suppression of the gap.

Now, we present the data of electrical resistivity $\rho_c(T)$ along the c axis of CeRhAs for $T>300$ K at various pressures in Fig. 2. The jump of ρ_c at T_1 results from the gap formation, as noted in the Introduction. The magnitude of the jump slightly increases with pressures, which is consistent with the increase of E_g/k_B along the c axis for $P<1$ GPa in Fig. 1(b). As shown in the inset of Fig. 2, the maximal temperature T_{max} in $\rho_c(T)$ around 300 K shifts to higher temperatures with a ratio of 110 K/GPa. The pressure dependence of T_{max} will be discussed below.

We move to the pressure dependence of $\rho_a(T)$ and $\rho_c(T)$ below 300 K. In Fig. 3, ρ_a at the lowest temperature hardly changes up to 1.6 GPa, but ρ_a decreases by two orders of magnitude on further increasing pressure from 1.6–3.1 GPa. For $P>2.3$ GPa, the metallic behavior appears below 70 K. On the other hand, the increase of ρ_c with P up to 1.6 GPa at low temperatures suggests the development of gap along the c axis. Above 1.9 GPa, however, ρ_c decreases significantly over the temperature range, and eventually exhibits a metallic behavior at 3.0 GPa. As shown in the inset, a crossover from $\rho_a(1.5\text{ K}) > \rho_c(1.5\text{ K})$ to $\rho_a(1.5\text{ K}) < \rho_c(1.5\text{ K})$ occurs at 1.5 GPa, implying a significant change in the electronic state of this compound.

In order to make clear the pressure dependence of the T_2 and T_3, the data of $\rho_a(T)$ and $\rho_c(T)$ in the range $50 \leqslant T \leqslant 250$ K are represented in Fig. 4. Steplike anomalies at both T_2 and T_3 in ρ_a and ρ_c shift to lower temperatures for $P \leqslant 1.6$ GPa and become broader, and vanish at 1.6 GPa. For $P \geqslant 1.6$ GPa, a weak anomaly appears at about $T^* \sim 230$ K in both ρ_a and ρ_c, and shifts to lower temperatures with pres-

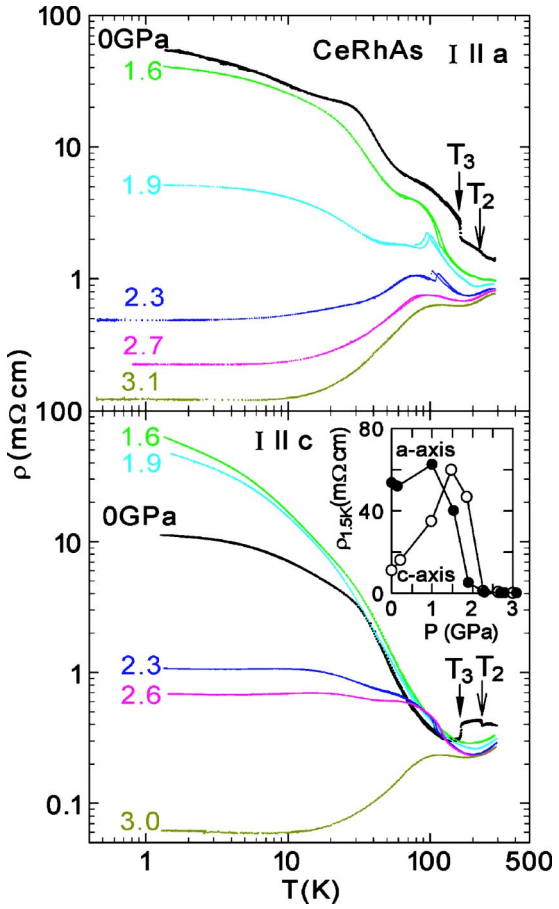

FIG. 3. (Color online) Temperature dependence of electrical resistivity ρ_a and ρ_c of CeRhAs for $I \| a$ and $I \| c$ under pressures up to 3.1 GPa.

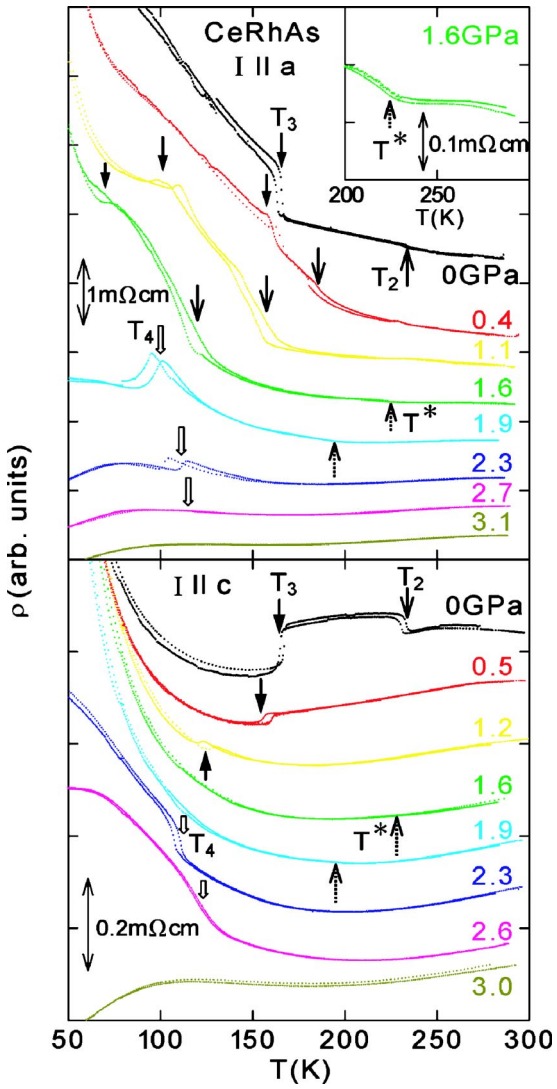

FIG. 4. (Color online) Temperature dependence of electrical resistivity ρ_a and ρ_c of CeRhAs for $50 \leqslant T \leqslant 300$ K under pressures. Data for each pressure are shifted by a constant value for clarity. The inset of the upper panel shows up the bend in $\rho_a(T)$ at T^*.

sure. For $P > 1.9$ GPa, a sharp peak in ρ_a and a jump in ρ_c with hysteresis manifest themselves at $T_4 \sim 100$ K, indicating a first-order phase transition. This transition shifts to higher temperatures with pressure and fades away at 3 GPa.

The pressure-induced transitions found in CeRhAs are expected to be related to structural transitions. Then, we measured the lattice parameters under pressures up to 2.5 GPa by powder x-ray diffraction. It is found that the orthorhombic ε-TiNiSi-type structure is sustained up to 2.5 GPa. Figure 5 shows the pressure dependence of lattice parameters and relative volume V/V_0 of CeRhAs at 250 K. It is noteworthy that the a parameter shrinks extremely with a ratio of -0.108 Å/GPa, while the b and c parameters slightly increase with the ratios of 0.0036 Å/GPa and 0.0093 Å/GPa, respectively. This elongation of b and c parameters by applying hydrostatic pressure is quite unusual and will be discussed later. By fitting Birch's equation[10] to the data of V/V_0 vs P, the bulk modulus B_0 was estimated to be 70 GPa, which is comparable with that reported for Ce based compounds such as $CeCu_6$ ($B_0 = 90$ GPa).[11]

The lattice parameters under pressures as a function of temperatures below 300 K was measured via the relative length change $\Delta L_a/L_a$ and $\Delta L_c/L_c$ along the a and c axes. The results are displayed in Fig. 6. It should be noted that the freezing of the pressure transmitting medium[12] gives rise to anomalies in both $\Delta L_a/L_a$ and $\Delta L_c/L_c$, as denoted by circles. These anomalies become pronounced peaks with increasing pressure, and shift to high temperatures with a ratio of 70 K/GPa as reported previously.[12] By contrast, the intrinsic anomalies at T_2 in both $\Delta L_a/L_a$ and $\Delta L_c/L_c$ become broader and shift to low temperatures with increasing pressure. On the other hand, the anomaly in $\Delta L_a/L_a$ at T_3 slightly shifts to high temperatures with increasing pressure up to 0.23 GPa with a ratio of 60 ± 20 K/GPa. This ratio agrees with 80 K/GPa which is estimated by Clausius-Clapeyron equation $dT/dP = \Delta V/\Delta S$, using $\Delta L_a/L_a = +0.2\%$, $\Delta L_c/L_c = -0.06\%$, and $\Delta L_b/L_b = -0.06\%$ from the previous x-ray diffraction data,[6] and $\Delta S = 0.35$ J/Kmol.[5] For $P \geqq 0.49$ GPa, however, the a parameter elongates and c parameter shrinks below T_3. Furthermore, both T_2 and T_3 decrease by applying pressure with a ratio of -100 K/GPa. For $P \geqq 1.5$ GPa, the steplike anomaly at T_3 vanishes suddenly. An upturn in $\Delta L_a/L_a$ and the associated decrease of $\Delta L_c/L_c$ appear at the temperature

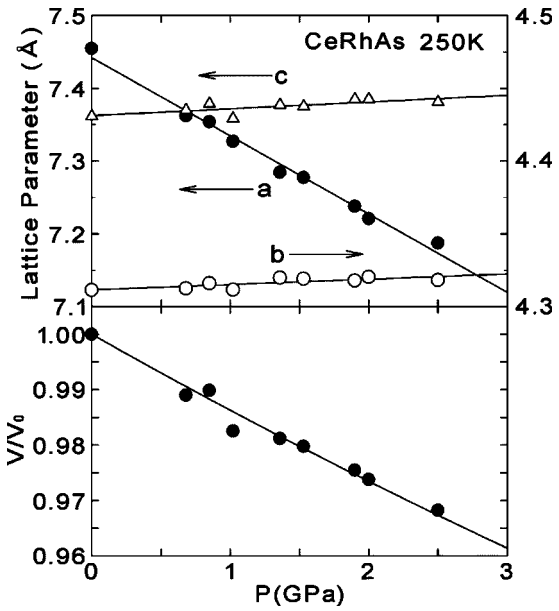

FIG. 5. Pressure dependence of lattice parameters and relative unit cell volume of CeRhAs at 250 K.

denoted by T^*, which shifts to low temperatures. The T^* is defined as the temperature where the thermal expansion dL/dT has a local minimum along the a axis and maximum along the c axis. For $P \geqq 1.9$ GPa, another phase transition at about $T_4 \sim 90$ K appears suddenly, and shifts to higher temperature with pressure.

The combination of the above results of electrical resistivity and thermal expansion suggests that CeRhAs undergoes phase transitions below T^* and T_4 at pressure above 2 GPa. In order to directly observe the structural transitions, we measured the temperature dependence of the powder x-ray diffraction at a fixed pressure of $P=2.1$ GPa. The diffraction-pattern profiles recorded at $T=300$ and 50 K (below T_4) are compared in Fig. 7. At first glance, almost same profiles suggest that neither structural type nor space group change on cooling below T_4. Looking more carefully, one notices some peaks split into two peaks with decreasing temperature. In Fig. 8, below 150 K$<T^*$, another peak of $(301)_{LT}$ appears at the lower angle side of the high-temperature peak $(301)_{HT}$. The $(301)_{LT}$ intensity grows in the consumption of the $(301)_{HT}$ intensity with decreasing temperature below 150 K. It means that the volume fraction of the phase with larger a parameter increases below T^*. Splitting of the peak was observed also for (400), (411), and (512). This splitting below T^* suggests the coexistence of two orthorhombic phases with slightly different a parameters.

IV. DISCUSSION

We now discuss the mechanism of the gap formation for CeRhAs based on the experimental data of the present work. So far, three scenarios have been proposed for the mechanism: (a) a charge ordering transition at T_1,[5] (b) a gap originated from c-f hybridization effect,[4,5,7,8] (c) a charge-

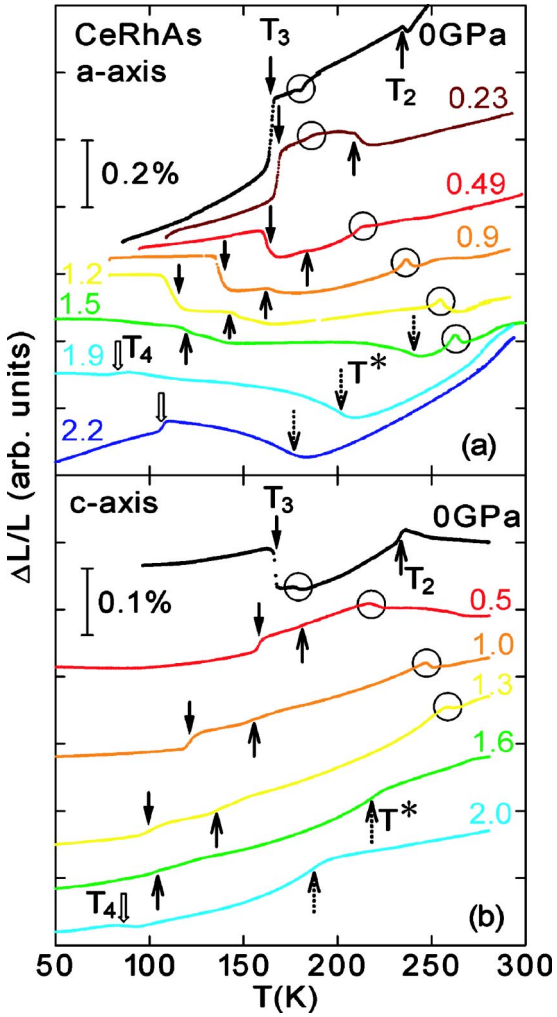

FIG. 6. (Color online) Temperature dependence of relative length change $\Delta L_a/L_a$ and $\Delta L_c/L_c$ along the a and c axis of CeRhAs under pressures. Data for each pressure are shifted by a constant value for clarity. The anomalies denoted by circles are due to the freezing of the pressure transmitting medium (Ref. 12).

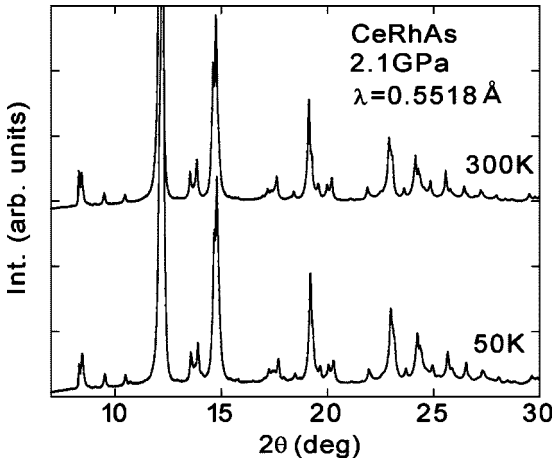

FIG. 7. Powder x-ray diffraction profiles of CeRhAs at 300 K and 50 K for $P=2.1$ GPa.

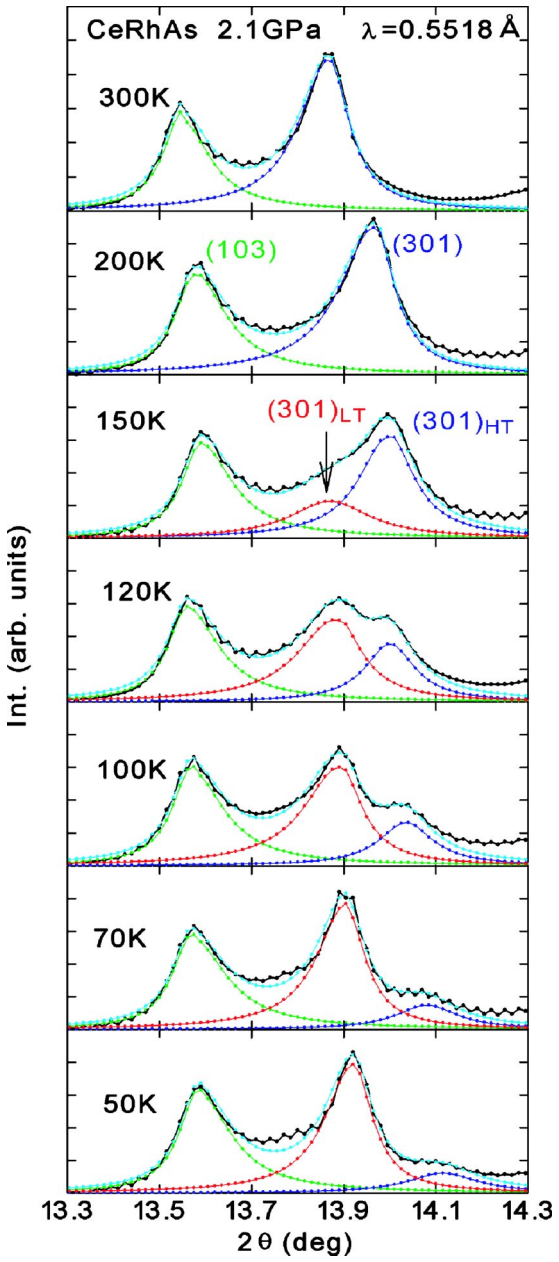

FIG. 8. (Color online) Temperature variations of powder x-ray diffraction profiles of CeRhAs around (103) and (301) lines for $P=2.1$ GPa.

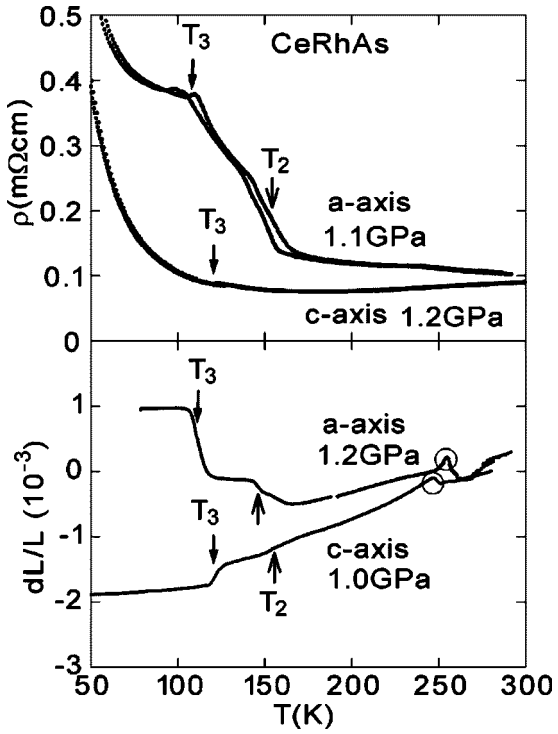

FIG. 9. Temperature dependence of electrical resistivity ρ_a and ρ_c and relative length change $\Delta L_a/L_a$ and $\Delta L_c/L_c$ of CeRhAs at about 1.1 GPa. The anomalies denoted by circles are due to the freezing of the pressure transmitting medium (Ref. 12).

density-wave (CDW) transition.[6] Our data cannot distinguish whether or not charge ordering occurs in CeRhAs. Therefore, we consider the scenarios (b) and (c). The c-f hybridization model[3] was applied to understand the pseudogap formation in the isostructural compounds CeNiSn and CeRhSb. According to this model, the hybridization gap Δ is given by $\Delta \propto T_K = 2z_{kB}V^2/D$, where z_{kB}, V, and D are the renormalization amplitude, hybridization matrix elements, and bare band width of conduction electrons, respectively. With increasing pressure, all z_{kB}, V, and D may increase. However, V^2/D should be enlarged with pressure because V is more sensitive to D. Therefore, the gap is expected to be enlarged with pressure, and scaled by T_K.[3] For CeRhSb, both the Kondo temperature T_K and the energy gap E_g/k_B increase with ratio of $d \ln T_K/dP = 0.30$ GPa^{-1} and $d(E_g/k_B)/dP = 5$ K/GPa with increasing pressure up to 3 GPa.[9] For many Ce compounds, the volume dependence of T_K, that is, Grüneisen parameter $\Gamma = -\partial \ln T_K/\partial \ln V = B_0 \partial \ln T_K/\partial P$ where B_0 is bulk modulus, is inversely proportional to T_K.[13] If the gap magnitude is increased by the enhancement of c-f hybridization, $d(E_g/k_B)/dV$ should be proportional to Γ and thus inversely proportional to T_K. Because $T_K = 1500$ K of CeRhAs is much larger than $T_K = 360$ K of CeRhSb, we expect that the $d \ln T_K/dP$ and $d(E_g/k_B)/dP$ for CeRhAs is much smaller than those for CeRhSb if B_0 is the same order for both compounds. Assuming T_K for CeRhAs to be proportional to T_{max}, the maximal temperature of ρ_c (see the inset of Fig. 2), then $d \ln T_{max}/dP = d \ln T_K/dP = 0.42$ GPa^{-1}. This value of $d \ln T_K/dP$ may be overestimated because the ρ_c near $T_{max} < T_1$ is affected by not only Kondo effect but also the gap opening at T_1. However, the fact that the value of $d(E_g/k_B)/dP = 27$ K/GPa along the c axis of CeRhAs is larger by a factor of 5 than that noted above for CeRhSb strongly suggests the different origin of gap formation.

In the previous paper,[4] it was argued that a reduction of the a-axis lattice parameter on cooling below T_1 would enhance the c-f hybridization, which leads to the formation and development of the gap in CeRhAs. This is an analogy with the case of CeNiSn, where uniaxial-pressure applied along the a axis enhances the hybridization and increases the gap magnitude.[14] For CeRhAs, however, the significant shrink along the a axis under pressure (see Fig. 5) is associated with

the decrease in E_g/k_B along the *a* axis (see Fig. 1). Another discrepancy is noticed by the comparison between the electrical resistivity ρ_a and thermal expansion $\Delta L_a/L_a$ along the *a* axis at $P \approx 1.1$ GPa shown in Fig. 9. Note that ρ_a increases on cooling below T_2 and T_3, regardless of the expansion along the *a* axis. Therefore, the simple scenario based on the *c*-*f* hybridization gap model seems to be not the case.

Second, we consider the CDW scenario. CDW gaps open at the Fermi surface at those portions that satisfy the nesting condition.[15] Figure 1 showed that the increase of the gap along the *c* axis of CeRhAs coincides with the increase of T_1 by applying pressure up to 0.5 GPa. We recall that the phase II below T_1 is characterized by the superlattice with modulation vector of $q_1=(0\ 1/2\ 1/2)$. This modulation should be related with the gap formation along the *c* axis. Nakajima *et al.* suggested that the lattice modulation is a result of a sort of CDW transition at T_1.[6] However, the transition temperature of conventional CDW materials decreases with pressure by the following reason. The CDW is formed if the gain in electronic energy resulting from the opening of the gaps exceeds the strain energy which increases with the formation of superlattice. The electronic-energy gain increases with decreasing temperature because the Fermi surface becomes sharper at low temperature. By applying pressure, the lattice stiffens in most cases, which increases the strain energy and destabilizes the CDW state. As a consequence, the CDW transition temperature is lowered under pressure, as observed in many cases. However, there are exceptions in which the transition temperature increases with pressure, although the reasons have remained unclear. The examples are a quasi-one-dimensional compound $ZrTe_3$,[16] a layered compound η-Mo_4O_{11},[17] and a filled skutterudite $PrRu_4P_{12}$.[18] The transition temperature can rise if the strain energy is reduced with pressure. As shown in Fig. 5, the increase of both *b* and *c* parameters of CeRhAs with pressure indicates the softening of the lattice in the *b*-*c* plane, which may reduce the strain energy. To confirm this scenario, elastic constant measurements under pressure are highly desirable.

Because CeRhAs is a three-dimensional compound, it seems that the nesting of the Fermi surfaces is difficult. Furthermore, the transition at T_1 is of first order as evidenced from the sharp peak in the specific heat of 90 J/mol K.[5] Although most of CDW systems are low dimensional, and undergo a second order transition, a first-order CDW transition was found in a few three-dimensional systems such as $Lu_5Ir_4Si_{10}$.[19] It was ascertained by a very narrow and huge cusp in the specific heat (150 J/mol K) at $T_c=80$ K. Furthermore, the energy gap E_g of 700 K for $Lu_5Ir_4Si_{10}$ is much larger than the value of $E_g=3.53k_BT_c$ derived from the weak coupling mean-field theory. This large gap was explained by a strong coupling model proposed by McMillan.[20] According to this model, a short coherence length leads to significant phonon softening, and eventually the relation $E_g>7k_BT_c$ is obtained. As mentioned above, CeRhAs shows a rather large cusp of 90 J/mol K in the specific heat at T_1. Furthermore, the value of $E_g/k_B=2000-4500$ K estimated by the measurement of Hall effect (Ref. 5) and optical reflectivity (Ref. 21) corresponds to 5–13 times of T_1, being far above the weak coupling value. These facts further support the conjecture that the transition at T_1 is a CDW transition of a strong electron-phonon coupling. To make sure this scenario, measurements of phonon dispersion by inelastic neutron scattering experiment are needed.

The transition of CeRhAs at T_1 is characterized by formation of a simple commensurate $(2b\times 2c)$ superlattice. This is also unusual because an incommensurate lattice modulation occurs in most of CDW compounds. The Hall coefficient of $1\sim 2\times 10^{-3}$ cm^3/C for CeRhAs above T_1 (Ref. 5) is one order of magnitude larger than the ordinary Hall coefficient of metallic intermediate-valence compounds such as CeNi, $CeSn_3$, and $CeRu_2$.[22] This suggests that the carrier concentration above T_1 is much smaller, that is, Fermi surface (FS) of CeRhAs is relatively small. In fact, the band structure calculation reveals the small gap opening above T_1.[23] In the calculated band structure for hexagonal CeRhAs, a flat band exists at the valence band top (Γ-*A* line). The cylindrical FS around the Γ point seems to be favorable for nesting relevant to a CDW transition. But, this FS is not consistent with the carrier concentration derived from the Hall coefficient measurement.[24] These features for the transition at T_1 of CeRhAs resembles the CDW transition in 1*T*-$TiSe_2$, which undergoes a commensurate $(2\times 2\times 2)$ transition at $T_C \sim 200$ K.[25] The normal phase of $TiSe_2$ above T_C is semimetal with a small Γ-point hole FS and *L*-point electron FS in the hexagonal Brillouin zone.[26] Because these FSs are difficult to nest each other, $TiSe_2$ does not fit into the conventional FS nesting model. To explain the unconventional CDW transition of this compound, a band Jahn-Teller mechanism was proposed.[27] Motizuki and co-workers developed a microscopic theory including the band Jahn-Teller mechanism. It was shown that the electron-phonon interaction as well as FS nesting plays an important role in the CDW transition in $TiSe_2$.[28] To make clear whether or not the transition of CeRhAs at T_1 is derived by the band Jahn-Teller mechanism, detailed study for the band structure near FS using an angle-resolved photoemission measurements is needed.

Next, we discuss the pressure dependence of T_2 and T_3 (see Fig. 1). The gradual decrease of T_2 and T_3 with increasing pressure above 0.2 GPa is consistent with that for the canonical CDW transition as discussed above. Below T_2 and T_3, the development of the gap is related to the superlattice formation with $q_3=(1/3\ 0\ 0)$. Here, the strain energy associated with this modulation increases by the shrink of the *a* parameter with pressure. Then, it is natural that the transition temperatures are lowered and the gap along the *a* axis is suppressed as shown in Fig. 1. However, the initial increase of T_3 for $P<0.2$ GPa contradicts this model. Probably, the other modulation with $q_2=(0\ 1/3\ 1/3)$ plays a role. To examine the relation between the development of the gap and lattice modulations, more detailed band structure calculation including the lattice modulations of q_2 and q_3 are necessary.

The most significant observation in the presence work is the sudden suppression of the gap of CeRhAs above 1.5 GPa. According to the band structure calculation,[23] the gap magnitude continues to increase with decreasing the *a* parameter down to 7.13 Å. Experimentally, the *a* parameter at 1.5 GPa is still 7.3 Å as shown in Fig. 5. Thus, the gap suppression cannot be explained by only a reduction of the *a* parameter. Instead, the gap closure should be related to the

appearance of the phase V below T_4. On going from the phase IV to phase V, the significant change of the electronic state is manifested in the reverse of anisotropy in the resistivity at low temperature, as shown in the inset of Fig. 3. The anomaly in resistivity at T_4 vanishes above 2.8 GPa, and then, the phase V seems to merge into the phase II. To examine the electronic state at high pressure above 3 GPa, microscopic experiments are needed.

V. SUMMARY

In summary, we have determined temperature-pressure phase diagram of "Kondo semiconductor" CeRhAs from resistivity, thermal expansion, and x-ray diffraction measurements using single crystalline samples. By applying pressure up to 1.5 GPa, T_1 increases with a ratio of 270 K/GPa, whereas both T_2 and T_3 decrease with a ratio of -100 K/GPa. The energy gap, which was estimated from the activation energy in the resistivity along the *c* axis, increases slightly with pressure up to 1 GPa, while that along the *a* axis decreases. Both gap energies vanish at approximately 2 GPa. The orthorhombic *a* parameter at 250 K decreases with pressure up to 2.5 GPa, while *b* and *c* parameters increase slightly. These findings suggest that the gap formation in CeRhAs is a result of a sort of CDW transition. The increase of T_1 under pressure may be explained by the strong-coupling CDW model. The CDW scenario provides better understanding of the unusual gap formation in CeRhAs, and this scenario needs to be examined by further studies of Fermi surfaces.

ACKNOWLEDGMENTS

We are grateful to F. Ishii to fruitful discussion. Resistivity and thermal expansion measurements were carried out at the Materials Science Center, N-BARD, Hiroshima University. The x-ray diffraction study at the BL-10XU in the SPring-8 was performed as a project (Proposal No. 2002A0469-ND2, 2002B0421-ND2, 2003A0248-ND2). This work was supported in part by a Grant-in-Aid for Young Scientists (Grant No. 15740217) and COE Research (Grant No. 13CE2002) from the Ministry of Education, Culture, Sports, Science and Technology of Japan.

*Electronic address: kumeo@sci.hiroshima-u.ac.jp

[1] T. Takabatake, F. Iga, T. Yoshino, Y. Echizen, K. Katoh, K. Kobayashi, M. Higa, N. Shimizu, Y. Bando, G. Nakamoto, H. Fujii, K. Izawa, T. Suzuki, T. Fujita, M. Sera, M. Hiroi, K. Maezawa, S. Mock, H. v. Löhneysen, A. Brückl, K. Neumaier, and K. Andres, J. Magn. Magn. Mater. **177-181**, 277 (1998).

[2] S. Yoshii, M. Kasaya, H. Takahashi, and N. Mōri, Physica B **223&224**, 421 (1996).

[3] H. Ikeda and K. Miyake, J. Phys. Soc. Jpn. **65**, 1769 (1996).

[4] T. Sasakawa, T. Suemitsu, T. Takabatake, Y. Bando, K. Umeo, M. H. Jung, M. Sera, T. Suzuki, T. Fujita, M. Nakajima, K. Iwasa, M. Kohgi, Ch. Paul, St. Berger, and E. Bauer, Phys. Rev. B **66**, 041103(R) (2002).

[5] T. Sasakawa, H. Miyaoka, K. Umeo, S. Aoyagi, K. Kato, F. Iga, and T. Takabatake, J. Phys. Soc. Jpn. **73**, 262 (2004).

[6] M. Nakajima, K. Iwasa, M. Kohgi, T. Sasakawa, and T. Takabatake, Acta Phys. Pol. B **34**, 1109 (2003).

[7] H. Kumigashira, T Sato, T. Yokoya, T. Takahashi, S. Yoshii, and M. Kasaya, Phys. Rev. Lett. **82**, 1943 (1999); H. Kumigashira, T. Takahashi, S. Yoshii, and M. Kasaya, *ibid.* **87**, 067206 (2001).

[8] T. Ekino, T. Takahashi, T. Suemitsu, T. Takabatake, and H. Fujii, Physica B **312-313**, 221 (2002).

[9] Y. Uwatoko, N. Mōri, G. Oomi, and J. D. Thompson, Physica B **239**, 95 (1997).

[10] F. F. Voronov, Sov. Phys. Dokl. **21**, 92 (1976).

[11] A. Shibata, G. Oomi, Y. Ōnuki, and T. Komatsubara, J. Phys. Soc. Jpn. **55**, 2086 (1986).

[12] K. Murata, H. Yoshino, H. O. Yadav, Y. Honda, and N. Shirakawa, Rev. Sci. Instrum. **68**, 2490 (1997).

[13] T. Kagayama, G. Oomi, E. Ito, Y. Ōnuki, and T. Komatsubara, J. Phys. Soc. Jpn. **63**, 3927 (1994).

[14] K. Umeo, T. Igaue, H. Chyono, Y. Echizen, T. Takabatake, M. Kosaka, and Y. Uwatoko, Phys. Rev. B **60**, R6957 (1999).

[15] G. Gruner, Rev. Mod. Phys. **60**, 1129 (1988); R. E. Peierls, *Quantum Theory of Solids* (Oxford University Press, London, 1955), p. 108; H. Fröhlich, Proc. R. Soc. London, Ser. A **223**, 296 (1954).

[16] K. Yamaya, M. Yoneda, S. Yasuzaki, Y. Okajima, and S. Tanada, J. Phys.: Condens. Matter **14**, 10767 (2002).

[17] S. Ohara, M. Koyano, H. Negishi, M. Sasaki, and M. Inoue, Phys. Status Solidi B **164**, 243 (1991).

[18] I. Shirotani, J. Hayashi, T. Adachi, C. Sekine, T. Kawakami, T. Nakanishi, H. Takahashi, J. Tang, A. Matsushita, and T. Matsumoto, Physica B **322**, 408 (2002).

[19] B. Becker, N. G. Patil, S. Ramakrishnan, A. A. Menovsky, G. J. Nieuwenhuys, J. A. Mydosh, M. Kohgi, and K. Iwasa, Phys. Rev. B **59**, 7266 (1999).

[20] W. L. McMillan, Phys. Rev. B **16**, 643 (1977).

[21] M. Matsunami, H. Okamura, T. Nanba, T. Suemitsu, T. Yoshino, T. Takabatake, Y. Ishikawa, and H. Harima, J. Phys. Soc. Jpn. **70**, 291 (2002).

[22] Y. Ōnuki, T. Yamazaki, T. Omi, I. Ukon, A. Kobori, and T. Komatsubara, J. Phys. Soc. Jpn. **58**, 2126 (1989).

[23] F. Ishii and T. Oguchi, J. Phys. Soc. Jpn. **73**, 145 (2004).

[24] F. Ishii (unpublished).

[25] F. J. Di Salvo, D. E. Moncton, and J. V. Waszczak, Phys. Rev. B **14**, 4321 (1976).

[26] A. Zunger and A. J. Freeman, Phys. Rev. B **17**, 1839 (1978); N. G. Stoffel, S. D. Kevan, and N. V. Smith, Phys. Rev. B **31**, 8049 (1985).

[27] H. P. Hughes, J. Phys. C **10**, L319 (1977).

[28] *Structural Phase Transitions in Layered Transition Metal Compounds*, edited by K. Motizuki (Reidel, Boston, 1986).